Influence of Resonances on Spectral Formation of X-Ray Lines In Fe XVII

Guo Xin Chen and Anil K. Pradhan
Department of Astronomy, The Ohio State University, Columbus, Ohio 43210
(February 1, 2008)

New theoretical results from large-scale relativistic close coupling calculations reveal the precise effect of resonances in collisional excitation of x-ray lines of Ne-like Fe XVII. Employing the Breit-Pauli R-matrix method and a 89-level eigenfunction expansion including up to $n = 4$ levels shows significant resonance enhancement of the collision strengths of forbidden and intercombination transitions. The present results differ from all previous calculations, heretofore without detailed resonance structures, and should help resolve longstanding discrepancies. In particular, the present line ratios of three benchmark diagnostic lines 3C, 3D, and 3E at 15.014, 15.265, and 15.456 $\AA$ respectively, are in excellent agreement with two independent measurements on Electron-Beam-Ion-Traps [Laming *et al.* , Astrophys. J **545**, L161 (2000) and Brown *et al.* , Astrophys. J **502**, 1015 (1998)]. The strong energy dependence due to resonances in these and other cross sections is demonstrated for the first time. It is of general importance and strongly manifests itself in x-ray plasma diagnostics.

PACS number(s): 34.80.Kw

Prominent Fe XVII x-ray lines have long been observed from laboratory and astrophysical sources [e.g. [3–5]], most recently in the *Chandra* and the *XMM-Newton* spectra of active galactic nuclei, x-ray binaries, supernovae, and flaring and non-flaring active stellar coronae [6,7]. In spite of a number of theoretical, experimental, and observational studies over decades there remain outstanding discrepancies related to atomic processes and astrophysical effects responsible for Fe XVII spectral formation in high temperature sources [1-15]. However, the interpretation of experimental and observational ratios of line intensities usually relies on collisional-radiative (C-R) models using theoretical cross sections that neglect the fundamental role of resonant excitation, which preferentially affects the forbidden and intercombination transitions as opposed to dipole allowed ones. Of particular interest are three prominent x-ray transitions to the ground level $1s^22s^22p^6\ {}^1S_0$ from excited levels: 3C (λ 15.014$\AA$) $1s^22s^22p^5[1/2]3d_{3/2}\ {}^1P^o_1$ (level 27), 3D λ 15.265$\AA$ $1s^22s^22p^5[3/2]3d_{5/2}\ {}^3D^o_1$ (level 23), and 3E λ 15.456$\AA$: $1s^22s^22p^5[3/2]3d_{5/2}\ {}^3P^o_1$ (level 17), (level numbers denote energy order relative to the ground level 1). While the 3C is dipole allowed, the 3D and 3E are spin-forbidden intercombination transitions. All but one of the previous calculations used the distorted wave (DW) approximation that neglects channel coupling, and hence resonances [8–11]. A point of confusion has been that the only previous coupled channel (CC) calculation [12] also yielded the same results as the DW calculations [11], because the CC R-matrix calculations were at energies *above all target levels in the eigenfunction expansion*; and therefore resonances were not included. Since both the DW and the CC results agreed, it has hitherto been assumed that resonance effects are not important, and that the cross sections are relatively constant with energy (e.g. [2,13]). On the other hand, the experiments on Electron-Beam-Ion-Traps (EBIT) at Lawrence Livermore National Laboratory (e.g. [2]), and at the National Institute of Standards and Technology (NIST, [1]), do not measure absolute excitation cross sections directly. Rather, they measure relative intensity ratios R1=3C/3D and R2=3E/3C at a few selected energies. Therefore the presence of resonances, and more generally the energy variations, are not readily discernible in experimental data (discussed later). The measured values differ from theoretical ones by up to 50% for R1, and a factor of 2 for R2 [1,2,13,14,6]. In order to accout for these discrepancies several mechanisms based on atomic and astrophysical effects have been put forward, such as polarization, resonance scattering, and dielectronic satellite blending, which may be of varying importance under appropriate conditions [1,2,7,15].

However, as evident from the results in this *Letter*, there are extensive resonance structures in cross sections for all transitions in Fe XVII due to many Rydberg series of resonances converging on to a number of $n = 3$ and $n = 4$ levels. Many infinite and interacting series of resonances arise due to coupling between open and closed scattering channels which, in principle, must be included in order to obtain the cross sections precisely. But for a complex ion such as Fe XVII the number of channels is very large and the CC calculations become enormously difficult, especially since relativistic fine structure must also be considered in addition to other atomic effects. Using the Breit-Pauli R-matrix (BPRM) method [16,17] we construct a large eigenfunction expansion including 89 levels corresponding to 49 LS terms up to the $n = 3$ and the $n = 4$ complexes of Fe XVII. Full details of the calculations will be presented elsewhere, but we briefly outline these below. The coupled-channel wavefunction expansion for the (e + Fe XVII) system may be expressed as $\Psi(E; \mathrm{e} + \mathrm{Fe\ XVII}) = \sum_i \chi_i(\mathrm{Fe\ XVII})\theta_\mathrm{e}(\ell_i) + \sum_j c_j\Phi_j(\mathrm{Fe\ XVI})$, where the Ψ denote the continuum (E > 0) states of given each total angular momemtum and parity Jπ, expanded in terms of the core ion eigenfunctions $\chi_i(S_iL_iJ_i)$; the $\theta_\mathrm{e}(\ell_i)$ refer to the free-electron partial wave, and the Φ_j are short-

range correlation functions that also serve to compensate for orthogonality constraints. The 89 levels belong to the configurations $2s^22p^6$, $2s^22p^5(3s,3p,3d)$, $2s^22p^5(4s,4p,4d,4f)$, $2s^12p^6(3s,3p,3d)$, $2s^12p^6(4s,4p,4d,4f)$. We consider total symmetries $2J \leq 51$ of both parities explicitly in the BPRM calculations. The size of the calculations (possibly the largest (e + ion) scattering calculations to date) may be gauged by the fact that the dimension of the Hamiltonian matrices ranges up to 10286, for J = 3.5 with 395 free channels and 486 bound channels (Φ_j) (the largest number of free channels per symmetry is 401); 25 continuum basis functions are used to represent the Ψ(e + Fe XVII) in the inner R-matrix region. Relativistic distorted wave (RDW) and Coulomb-Born-Bethe approximations are employed to 'top-up' the partial wave summations. Particular attention is paid to the resolution of resonances, with cross sections computed at about 20,000 energies.

Figs. 1(a-c) display the dense resonance structures in excitation collision strengths for the 3C, 3D, and 3E transitions respectively. The results are compared with the RDW values (filled circles, [8]) that essentially represent previous DW calculations (such as from the HULLAC code [9,10]), and the one *non-resonant* value from the previous CC R-matrix calculation (filled square, [12]). As seen from the figures, the other data correspond roughly to the 'background' collision strength compared to the present detailed results. The energy behavior of the three transitions may be ascertained from the eigenfunction expansions of the upper levels: 3C: $0.7857|27\rangle + 0.1753|23\rangle + 0.0305|17\rangle$, 3D: $0.7479|23\rangle + 0.2010|27\rangle + 0.0491|17\rangle$, and 3E: $0.9150|17\rangle + 0.0767|23\rangle + 0.0030|27\rangle$, where the eigenkets correspond to the energy level indices. As the mixing coefficients indicate the 3D has a significant component of $|^1\mathrm{P^o}\rangle$, but the 3E considerably less so. Therefore the 3D would depart from LS coupling to intermediate coupling to jj-coupling schemes along the neon isoelectronic sequence with Z, *and with* Ω(3D) *increasing with energy* like Ω(3C). On the other hand the 3E remains largely a (spin) forbidden transition and Ω(3E) decreases with energy. The Einstein A-coefficients of the 3C, 3D, and 3E are $2.47 \times 10^{13}, 6.01 \times 10^{12}$, and 9.42×10^{10} sec^{-1} respectively. Other interesting atomic physics aspects of these and other transitions in neon-like ions will be discussed in later publications, with particular reference to laser transitions.

Spectral formation in laboratory and astrophysical plasmas needs to be distinguished from each other. While we describe the latter using a C-R model for Fe XVII, generally using collision strengths averaged over a Maxwellian characterizing a temperature, the former are measured using a mono-energetic beam with a certain veocity spread assumed to be a gaussian. We compute the collision strengths averaged three ways: (i) Maxwellian, (ii) gaussian, and (iii) numerical. Present results for (ii) and (iii) are shown in Figs. 1(a-c). In order to compare with EBIT experiments the gaussian FWHM is taken to be 30 eV. We note that the energy variations, dependent on resolution and density of resonances in a given energy region, are reflected in the gaussian averages (ii); the numerical averages are slowly varying. The theoretical line ratios using gaussian and numerical averages $\langle\sigma\cdot v\rangle$ (GA and NA respectively; σ denotes the cross section), are computed taking account of the radiative branching ratios for 3C, 3D, and 3E which are: 1.0, 1.0, and 0.89 respectively. Therefore we have $R1 = 3\mathrm{C}/3\mathrm{D} = \langle\sigma_{3\mathrm{C}}\cdot v\rangle/\langle\sigma_{3\mathrm{D}}\cdot v\rangle$ and $R2 = 3\mathrm{E}/3\mathrm{C} = 0.89\langle\sigma_{3\mathrm{E}}\cdot v\rangle/\langle\sigma_{3\mathrm{C}}\cdot v\rangle$. The results are compared with several EBIT measurements in Table I. These direct theoretical results agree with measured values to within experimental errors. Although our calculations extend up to the $n = 4$ levels, the highest threshold (level 89) is at ∼84.5 Ryd or 1.15 keV; no resonances above this energy are therefore included. While the line ratios at 0.85 keV and 0.9 keV are computed directly from the collision strengths as in Figs. 1(a-c), some extrapolation of the averaged values is made to compare with the experimental value at 1.15 keV since we expect similar resonance enhancement above the $n = 4$ due to still higher thresholds. The GA results differ rather more than the NA results but still agree with experiment, in contrast to all other theoretical values. However, there is significant variation with energy in the GA collision strengths as they 'oscillate' irregularly with energy depending on the density of resonances prevalent in a given range. This appears to be reflected in similar 'oscillatory' structure seen in the experimental values reported in [14] throughout the energy range 0.1 - 4 keV.

TABLE I. Comparison of present line ratios for R1=3C/3D and R2=3E/3C with EBIT measurements

		E_i=0.85 keV	0.9 keV	1.15 keV
	EBIT	2.77±0.19[a]	2.94±0.18[b]	(3.15±0.17,2.93±0.16)[a]
R1=3C/3D	Theory[c]:NA	2.80	3.16	3.05[†]
	Theory[c]:GA	2.95	3.27	3.10[†]
	Other Theory		3.78[d];4.28[e];3.99[f]	
	EBIT		0.10±0.01[b]	
R2=3E/3C	Theory[c]:NA	0.11	0.085	0.07[†]
	Theory[c]:GA	0.11	0.083	0.07[†]
	Other Theory		0.04[d];0.05[e];0.05[f]	

[a] EBIT experiments at LLNL [2]; [b] EBIT experiments at NIST [1]; [c] present theory with NA and GA; [d] [8]; [e] [11];

^{f} [12]; †present values with extrapolation of resonance enhancement from *ab initio* collision strengths from E $\leq$ 1.02 keV (see text).

We also find that it is the $n = 4$ resonances, rather than the $n = 3$, that dominate the enhancement of electron impact cross sections in Fe XVII. The $n = 4$ resonances begin with resonant configurations $2s^2 2p^5 3\ell 4\ell'$ that manifest themselves from ∼47 Ryd, considerably *below* the excitation thresholds of the 2p $\longrightarrow$ 3d lines 3C, 3D, and 3E at ∼60 Ryd. Therefore there are relatively fewer $n = 3$ resonances and the $n = 4$ resonances greatly influence the near-threshold behavior of these cross sections. In the region 75 - 84.5 Ryd the resonances are due to thresholds corresponding to two-electron-excitation configurations $2s2p^6 4\ell$ with weakly coupled channels and resonances. This region is expected to be dominated by $n > 4$ resonances. It might also be mentioned that radiation damping of autoionizing resonances in cross sections of Fe XVII is known to be negligible [18–20].

We note a few specific cases that exemplify the findings in this *Letter*. An application of the present rates would be to estimate more preciesly the degree of resonance scattering of the 15.014 $\mathring{A}$ line in the solar and stellar coronae as discussed in [1,13]. Based on our C-R model with the present collisional data and extensive new radiative calculations for Fe XVII transition probabilities using the BPRM method (as in [21]) and from the SUPERSTRUCTURE code [22], we obtain the 3C/3D ratio to vary between 2.63 - 3.20, which agrees with the values from EBIT and from flaring solar corona, but is still higher than the observed value [15] of 1.87±0.21 from non-flaring active region. This further suggests that resonance scattering of 3C, or possibly some other mechanism, may be operative under astrophysical conditions [1]. Another example is the discussion of the diagnostic utility of the 3C/3D line ratio by Brown *et al.* [13] who (a) assume the cross sections to be relatively constant, and (b) mutiply the RDW cross section of Zhang and Sampson by 1.25 to agree with the measured value. From the present work neither (a) nor (b) are necessary. Furthermore, Brown *et al.* obtain the temperature dependence of 3C/3D including an inner-shell satellite line blended with the 3D, but using constant cross sections. A revised analysis with the present cross sections should yield a different temperature diagnostics.

More generally, the excitation of most of the $n = 3$ levels of Fe XVII is similarly affected. Using our 89-level C-R model, with newly computed collsional and radiative data employing the BPRM method, we investigated the prominent transitions corresponding to the 'coronal' X-ray lines $2s^2 2p^5 3s \longrightarrow 2s^2 2p^6$ at $\lambda\,\lambda$ 16.780, 17.055 and 17.100 $\mathring{A}$ (e.g. [23]). Fig. 2(a) shows the detailed collision strength for the forbidden J = 1 $\longrightarrow$ 0 λ 16.780 $\mathring{A}$ (3F) transition, compared with previous DW values (filled circles [8] and square [11]). The forbidden transitions are expected to be most enhanced by resonances, as in Fig. 2(a), since the background cross sections are much smaller than for allowed transitions. The temperature dependence of the forbidden (3F) to the allowed (3C) line ratio R3 = 3F/3C = I(16.780)/I(15.014) is demonstrated in Fig. 2(b), and compared with that calculated using DW cross sections (filled squares [11]); at higher temperatures the resonance contribution decreases progressively with energy due to the Maxwellian factor. The electron density dependence is small; solid-line and dot-line correspond to 10^{13} and 10^9 cm^{-3} respectively. The 4 open circles with error bars are observed and experimental values. At all temperatures T $< 10^7$ K the present line ratio departs considerably from those using DW data without resonances, to more than a factor of 3 at about 10^6 K—a fact of considerable importance in photoionized X-ray plasmas that have temperatures of maximum abundance much lower than that in coronal equilibrium $T_m \sim 4 \times 10^6$ K for Fe XVII, as marked.

TABLE II. Rate coefficients at T_e=200 eV for resonant excitation to the $2s^2 2p^5 3s$ levels

final		Rate Coefficient ($\times 10^{-13}$cm^{3}sec^{-1})		
state	Present	Smith *et al.* [4]	Goldstein *et al.* [9]	Chen&Reed [10]
$2p^5 3s\ ^3\mathrm{P}^o_1$	22.7	48.0	15.12	14.2
All 2p^{5}3s states	70.4	147.0	46.68	42.7

Resonant excitation may be considered indirectly by approximate methods such as quantum defect theory [20] or isolated resonance approximations (IRA) [4,9,10]. Table II compares the present rate coefficients for the individual 3F line, and for all transitons to the $2s^2 2p^5 3s$ levels, with IRA calculations using HULLAC [9], multi-configuration Dirac-Fock [10], and semi-relativistic Hartree-Fock [4] methods. The present data are ∼50% higher and differ from [9,10] which (i) neglect interference between resonances, and (ii) take limited account of the several infinite Rydberg series of resonances resulting in a considerable underestimate of resoance enhancement. The imprecision of the IRA is also indicated by more than a factor of 3 discrepancy between [10] and [4], both using IRA but with different decay channels. Present results are about a factor of 2 lower than [4]. Although resonances are generally less important for highly charged ions, the resulting enhancement in the BP R-matrix cross sections for forbidden and intercombination lines, compared to the allowed line, yields the ratios R1 and R2 closer to experiments compared to other works. We also note that ionization and recombination processes are not included in the present C-R model; dielectronic recombination from Fe XVIII to Fe XVII may also contribute to line emissions.

The main conclusions of this *Letter* are: (I) resonances are present in Fe XVII collision cross sections at all energies, (II) the energy dependence of different types of forbidden, intercombination, and allowed spectral transitions is demonstrated, (III) the effect on diagnostic line ratios is significant, and may be up to several factors compared to previous data neglecting resonance effects, (IV) the present work is expected to be generally applicable to the temeprature and density analysis of many astrophysical and laboratory X-ray sources (especially photoionized plasmas and forbidden lines) not only for Fe XVII but also other neon-sequence ions of importance in X-ray lasers [24], (V) this work is part of a large-scale program to compute excitation, photoionization, (e + ion) recombination [19,20], and transition probabilities of Fe XVII using the accurate BPRM method; for example, a set of A-values for ∼30 000 transitions have been computed.

We would like to thank Dr. Werner Eissner for assistance with the Iron Project BPRM codes. This work was partially supported by the National Science Foundation and the NASA Astrophysical Theory Program. The computational work was carried out utilising well over 1000 CPU hours on the Cray YMP, T94, and SV1 at the Ohio Supercomputer Center in Columbus Ohio.

---

[1] J.M. Laming *et al.* , Astrophys. J. (Lett.) , **545**, L161 (2000)
[2] G.V. Brown, P. Beiersdorfer, D.A. Liedahl, and K. Widmann, Astrophys. J. , **502**, 1015 (1998)
[3] J.C. Raymond and B.W. Smith, Astrophys. J. , **306**, 762 (1986); N.S. Brickhouse, J.C. Raymond, and B.W. Smith, Astrophys. J. Suppl. , **97**, 551 (1995)
[4] B.W. Smith, J.C. Raymond, J.B. Mann, and R.D. Cowan, Astrophys. J. , **298**, 898 (1985)
[5] R.F. Hutcheon, F.P. Paye and K.D. Evans, Mon. Not. R. Astron. Soc. , **175**, 489 (1976)
[6] C.R. Canizares *et al.* , Astrophys. J. (Lett.) , **539**, L41 (2000)
[7] J.L.R. Saba, J.T. Schmelz, A.K. Bhatia, and K.T. Strong, Astrophys. J. , **510**, 1064 (1999);
[8] H.L. Zhang and D.H. Sampson, At. Data Nucl. Data Tables, **43**, 1 (1989)
[9] W.H. Goldstein, A. Osterheld, J.Oreg, and A. Bar-Shalom, Astrophys. J. (Lett.) , **344**, L37 (1989)
[10] M.H. Chen and K.J. Reed, Phys. Rev. A , **40**, 2292 (1989)
[11] A.K. Bhatia and G.A. Doschek, At. Data Nucl. Data Tables, **52**, 1 (1992); M.Cornille, J. Dubau, F. Faucher, F. Bely-Dubau, and C. Blancard, Astron. Astrophys. Suppl. , **105**, 77 (1994); O. Bely and F. Bely, Sol. Phys., **2**, 285 (1967)
[12] M. Mohan, R. Sharma, and W. Eissner, Astrophys. J. Suppl. , **108**, 389 (1997)
[13] G.V. Brown, P. Beiersdorfer, H. Chen, and K.J. Reed, Astrophys. J. (Lett.) , **557**, L75 (2001)
[14] G.V. Brown, P. Beiersdorfer, and K. Widmann, Phys. Rev. A , **63**, 032719 (2001)
[15] K. Waljeski, *et al.* , Astrophys. J. , **429**, 909 (1994)
[16] D.G. Hummer, K.A. Berrington, W. Eissner, A.K. Pradhan, H.E. Saraph and J.A. Tully, Astron. Astrophys. **279**, 298 (1993).
[17] K.A. Berrington, W. Eissner, and P. H. Norrington, Comput. Phys. Commun. **92**, 290 (1995).
[18] A.K. Pradhan and H.L. Zhang, J. Phys. B **30**, L571 (1997).
[19] A.K. Pradhan, S.N. Nahar, and H.L. Zhang, Astrophys. J. (Lett.) **549**, L265 (2001).
[20] H.L. Zhang, S.N. Nahar and A.K. Pradhan, Phys. Rev. A **64**, 032719-1 (2001).
[21] S.N. Nahar and A.K. Pradhan, Physica Scripta **61**, 675 (1999).
[22] W.B. Eissner, M. Jones and H. Nussbaumer, Comput. Phys. Commun. , **8**, 270 (1974)
[23] C.W. Mauche, D.A. Liedahl, and K.B. Fournier, astro-ph/0106518 (2001).
[24] M.D. Rosen, P. Hagelstein, D.L. Matthews, E.M. Campbell, A.U. Hazi, B.L. Whitten, B. MacGowan, R.E. Turner, R.W. Lee, G. Charatis, G.E. Busch, C.L. Shepard, and P.D. Rochett, Phys. Rev. Lett. **54**, 106 (1985)

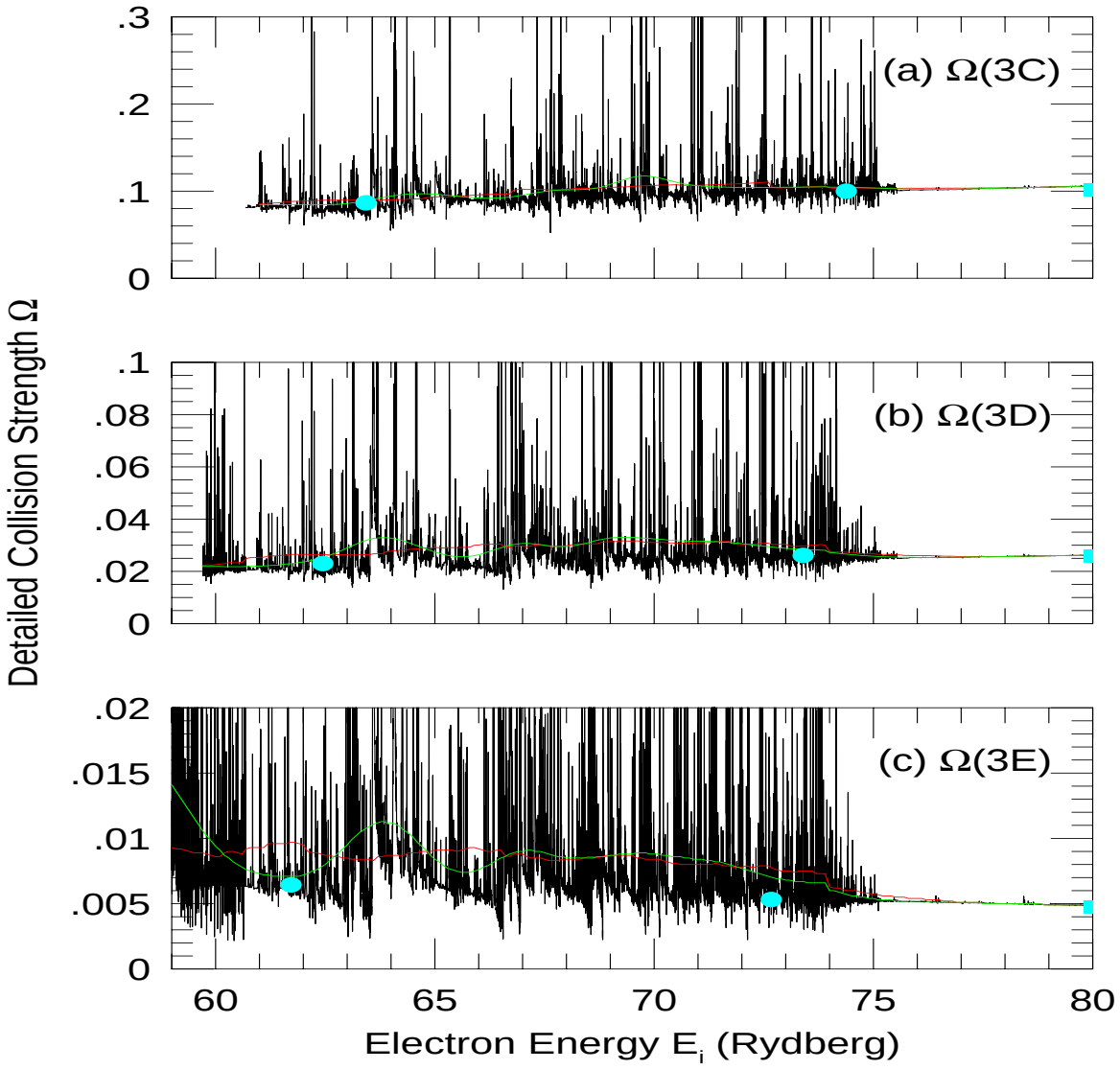

FIG. 1. Breit-Pauli R-matrix collision strength Ω for 3C, 3D and 3E lines with detailed resonance structures as a function of incident electron energy; filled dots are RDW results. The gaussian (FWHM = 30 eV) and numerical averages are also shown (see text).

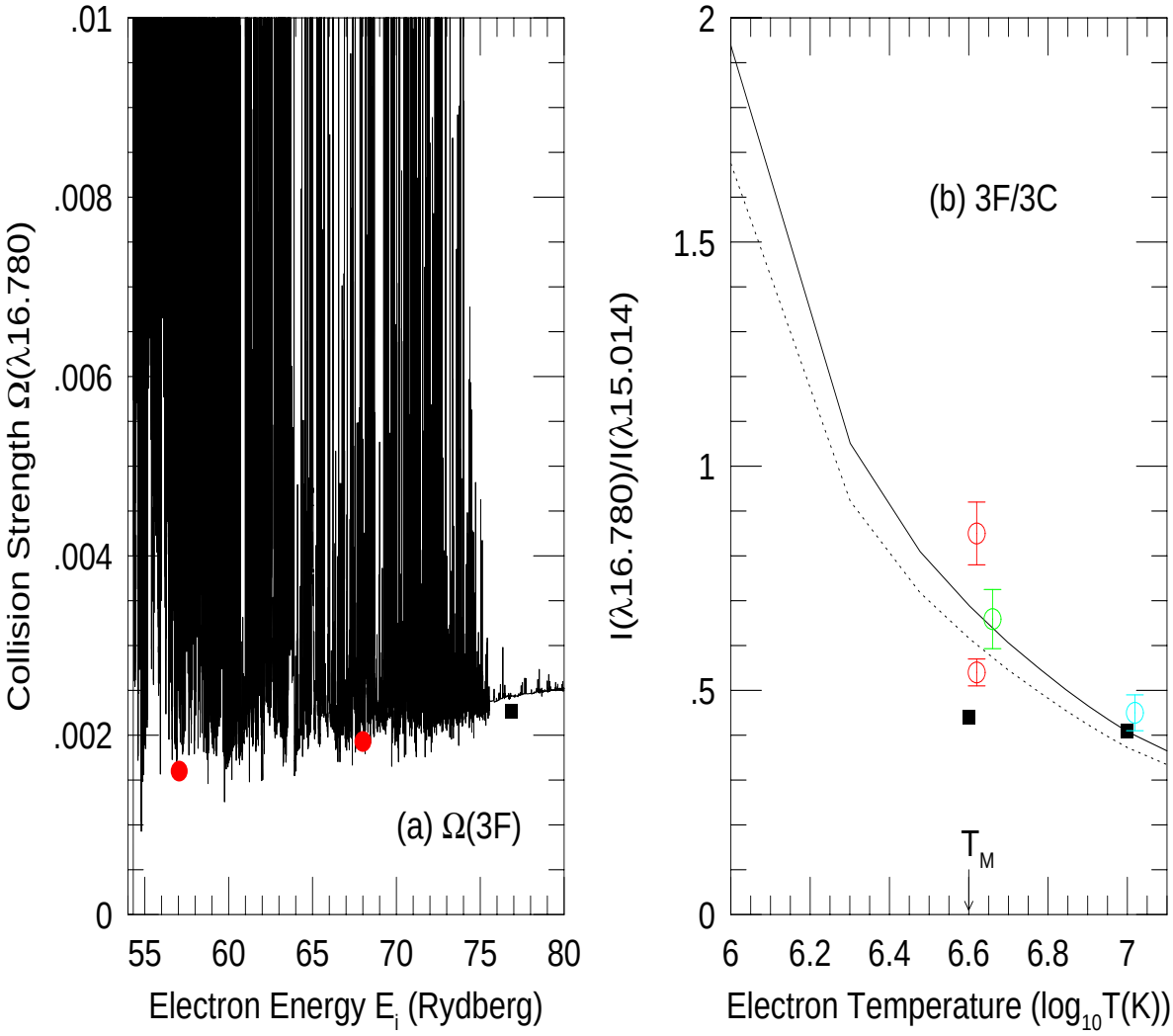

FIG. 2. (a): Breit-Pauli R-matrix collision strength Ω for the 3F line; the filled circles and square are non-resonant DW calculations; (b): line ratio 3F/3C vs. T from a 89-level C-R model. The electron densities for solid-line and dot-line curves are 10^{13} and 10^{9} cm^{-3} respectively. The 4 open circles with error bars are observed and experimental values: from the solar corona at $T_m \sim$ 4MK [5], from the corona of solar-type star Capella at $\sim$ 5MK [6], and from the EBIT experiment at 0.9 keV (log T = 7) [1]. The filled squares are values using DW results [11].